PERIODICA POLYTECHNICA SER. TRANS. ENG. VOL. 21, NO. 1, PP. 37-53 (1993)

ON TORSIONAL ELASTIC WAVES IN THE VEHICLE GEARED DRIVE SYSTEMS

Roman BOGACZ and Tomasz SZOLC

Institute of Fundamental Technological Research
Polytechnika Krakowska, Institute of Railway Vehicles
35155 Krakow 41. Warsawszka 24
Warsaw, Poland

Received: 10. November 1992

Abstract

In the paper, non-linear transient torsional vibrations of the motor and rail vehicle drive systems are investigated. Considerations are performed using discrete-continuous models consisting of rigid bodies of constant and variable mass moments of inertia connected each other by means of cylindrical elastic elements with continuously distributed parameters as well as by means of massless, non-linear torsional springs. An application of the d'Alembert solutions of the wave motion equations leads to appropriate systems of linear and non-linear ordinary differential equations with a 'shifted' argument. The shifted argument enables to solve these systems of equations numerically in an appropriate sequence which, in comparison with coupled ordinary differential equations for analogous discrete models, essentially increases the numerical efficiency and accuracy of the proposed method. In the numerical examples, there are considered some non-linear effects due to backlashes in the geared drive systems of the motor vehicle and the electric locomotive bogie.

Keywords: dynamics of machines, torsional vibrations

1. Introduction

Drive systems belong to the most heavily affected and responsible elements of the rail and motor vehicles. The drive systems usually consist of a driving motor, i. e. the internal combustion reciprocating engine in the case of a motor vehicle, or the electric motor in the case of a rail vehicle, elastic couplings, dry friction clutch, gear stages, joints and driven wheels. All these elements are connected by shaft segments. During the operation of the vehicle, the drive system elements rotate and they are usually affected by torsional, lateral, longitudinal and circumferential vibrations. These vibrations are a source of the most important dynamic loads of the individual drive system elements. A high-frequent alternation of dynamic torques of stresses transmitted by the individual drive system elements can cause dangerous fatigue cracks or can be a source of unnecessary noise generation. As it follows from [1 – 6], for dynamic investigations of the rail and motor vehicle drive systems, the torsional vibrations are predominant and

couplings with the remaining kinds of vibrations can often be neglected. Nevertheless, dynamic phenomena associated with vibrations of the drive systems, especially with torsional vibrations, are complicated in character. Complex characteristics of the elastic couplings, dry friction effects in clutches and brakes, backlashes in the gear stages, variations of the gear mesh stiffnesses, additional kinematic excitations due to the Cardan universal joints, wear of contact surfaces and their manufacture errors as well as a complex character of damping have significant influence on vibrations of the whole drive system making them non-linear.

In order to determine the drive system's maximum amplitudes and a time history of transient or steady-state forced vibrations, it is necessary to perform numerical simulations based on an appropriate mechanical and mathematical model. Computer simulations of the vehicle drive systems to analyze torsional vibration effects are mostly based on a discrete mechanical model described by simultaneous, i. e. coupled, non-linear ordinary differential equations. In order to obtain system dynamic response, a direct numerical integration of these equations is required [1 – 6].

Although a number of numerical methods and algorithms have been developed so far, there are still essential problems with solving this kind of equations, particularly in the engineering routine aspect. As it follows from [1, 5, 7, 8], a direct numerical integration of coupled ordinary differential equations is usually time-consuming, even for computers of the 'work-station' type which are commonly used in industrial research laboratories and technological scientific centres. Moreover, the so far applied numerical methods of integration of the non-linear, coupled ordinary differential equations describing torsional vibrations of the vehicle drive systems can often bring about significant errors, particularly in the case of investigations into gear tooth impacts due to backlashes [1, 4, 5].

In order to overcome the above mentioned difficulties connected with numerical simulations of torsional vibrations of the rail and motor vehicle drive systems by using the methods applied so far, in the paper an alternative approach is proposed. This approach is based on a discrete-continuous (hybrid) mechanical model of the drive system and on the wave interpretation of torsional vibrations. Investigations into the vehicle drive systems will focus on dynamic phenomena in the gear stages.

2. Assumptions and Formulation of the Problem

In the paper, there is considered a motor or rail vehicle drive system which consists of a driving motor, i. e. a reciprocating engine or an electric motor, elastic coupling with a dry friction clutch, gear stages, Cardan universal

joints and driven vehicle masses. *Fig. 1* presents a discrete mechanical model of this drive system. This model is a combination of $n + 2m + l + 2$ rigid bodies of constant and variable mass moments of inertia I_i, $i = 1, 2, \ldots, n+m+l+2$, representing the masses of the engine auxiliary drive elements or those of the electric motor rotor, respectively, n crank assemblies, flywheel, coupling halves, gear wheels, joint elements and $l+1$ driven vehicle masses. These rigid bodies are connected by massless torsional springs of constant stiffnesses k_j, $j = 1, 2, \ldots, n+m+l+1$, representing shaft segments as well as by means of m massless torsional springs of variable stiffnesses h_k, $k = n+2, n+3, \ldots, n+m+1$, representing torsional flexibilities of the elastic coupling, gear stage meshings and the Cardan universal joints, *Fig. 1*.

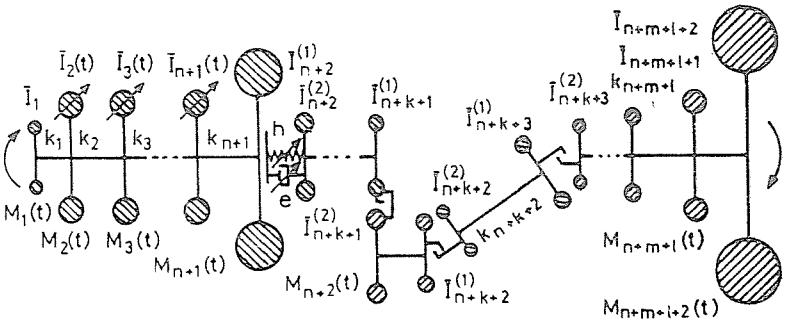

Fig. 1. Discrete model of the drive system

Internal and external dampings in the system are represented by a linear model of viscous type except the elastic coupling and the gear stages, for which non-linear damping terms are introduced [1, 4]. The considered system is excited to vibrations by active external torques $M_j(t)$, $j = 1, 2, \ldots, n+1$, as well as by constant or variable passive external torques $M_k(t)$, $k = n+2, n+3, \ldots, n+m+l+2$. Motion of the discrete model is described by the above mentioned appropriate system of linear and non-linear simultaneous ordinary differential equations, which can be found in [1, 8].

In order to avoid the mentioned numerical difficulties connected with integration of these equations, for the considered drive system an alternative discrete-continuous (hybrid) mechanical model is introduced. This model consists of the same number of rigid bodies like the discrete one, but the shaft segments of constant torsional flexibilities are represented by torsionally deformable cylindrical elastic elements with continuously distributed parameters of lengths l_i and identical stiffness values k_i, $i = 1, 2,$

$\ldots, n+m+l+1$, (*Fig. 2.*) Only torsional flexibilities of the elastic coupling, gear stage meshings and the Cardan universal joints are represented by the massless springs of the same variable stiffnesses h_j, $j = n+2, n+3, \ldots, n+m+1$. The constant components of mass moments of inertia of the hybrid model rigid bodies are determined by using the proper parameter identification procedure [9] in order to keep total mass moment of inertia of the system unchanged and to obtain possibly small differences of the corresponding first natural frequencies and mode shape functions in comparison with those of the discrete model. The external torques as well as the variable components of the mass moments of inertia are described by identical functions as in the case of discrete model. Moreover, in the hybrid model also external and internal dampings are assumed in the form of analogous concentrated linear and non-linear damping moments imposed on extreme cross-sections of the continuous elastic elements [7, 8, 10, 11].

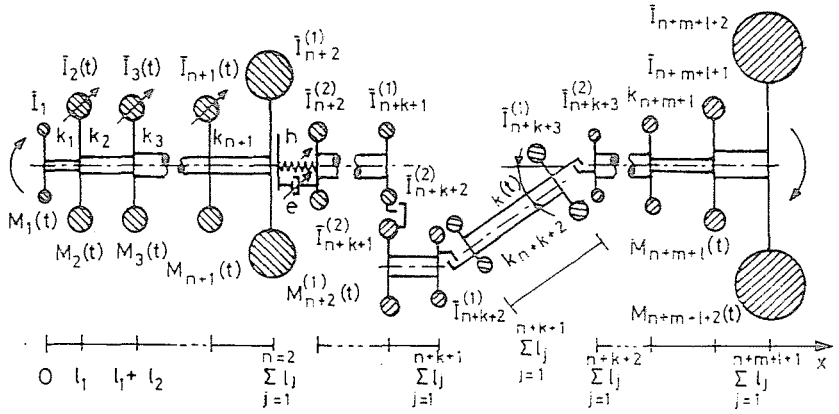

Fig. 2. Discrete-continuous model of the drive system

Equations of motion for angular displacements of the elastic element cross-sections of the hybrid model are classical wave equations

$$a^2\Theta_{i,xx}(x,t) - \Theta_{i,tt}(x,t) = 0\,, \qquad i = 1, 2, \ldots, n+m+l+1\,, \tag{1}$$

where: $a^2 = G/\rho$ and x are spatial coordinates parallel to the system rotation axis, (*Fig. 2.*) These equations are solved with appropriate initial conditions and with following boundary conditions

$$I_1\Theta_{1,tt} + d_1\Theta_{1,t} - c_1 l_1 \Theta_{1,xt} - k_1 l_1 \Theta_{1,x} = M_1(t) \qquad \text{for } x = 0\,,$$

$$I_i(\Theta_i)\,\Theta_{i,tt} + [d_i + 0.5\Theta_{i,t}L_i(\Theta_i)]\,\Theta_{i,t} + c_{i-1}l_{i-1}\Theta_{i-1,xt} - c_i l_i \Theta_{i,xt} +$$
$$+k_{i-1}l_{i-1}\Theta_{i-1,x} - k_i l_i \Theta_{i,x} = M_i(t)\,,$$

$$\Theta_{i-1} = \Theta_i\,, \qquad i = 2,\,3,\,\ldots\,,n+1, \qquad \text{for } x = \sum_{j=1}^{i-1} l_j\,,$$

$$I_k^{(1)}\Theta_{k-1,tt} + d_k^{(1)}\Theta_{k-1,t} + c_{k-1}l_{k-1}\Theta_{k-1,xt} + \alpha_k e_k(\Delta\Theta_k(t))$$
$$[\alpha_k\Theta_{k-1,t} - \beta_k\Theta_{k,t}] + k_{k-1}l_{k-1}\Theta_{k-1,x} + \alpha_k h_k(\Delta\Theta_k(t))$$
$$[\alpha_k\Theta_{k-1} - \beta_k\Theta_k] = M_k^{(1)}(t)$$

and

$$I_k^{(2)}\Theta_{k,tt} + d_k^{(2)}\Theta_{k,t} - c_k l_k \Theta_{k,xt} + \beta_k e_k(\Delta\Theta_k(t))\,[\alpha_k\Theta_{k-1,t} - \beta_k\Theta_{k,t}] -$$
$$-k_k l_k \Theta_{k,x} - \beta_k h_k(\Delta\Theta_k(t))\,[\alpha_k\Theta_{k-1} - \beta_k\Theta_k] = M_k^{(2)}(t)\,, \qquad (2)$$
$$\Delta\Theta_k(t) = \alpha_k\Theta_{k-1} - \beta_k\Theta_k$$
$$\text{for } x = \sum_{j=1}^{k-1} l_j\,, \qquad k = n+2,\,n+3,\,\ldots\,,n+m+1\,,$$

$$I_j\Theta_{j,tt} + d_j\Theta_{j,t} + c_{j-1}l_{j-1}\Theta_{j-1,xt} - c_j l_j \Theta_{j,xt} + k_{j-1}l_{j-1}\Theta_{j-1,x} -$$
$$-k_j l_j \Theta_{j,x} = M_j(t)\,,$$

$$\Theta_{j-1} = \Theta_j\,, \qquad j = n+m+2,\,n+m+3,\ldots\,,nml1, \qquad \text{for } x = \sum_{i=1}^{j-1} l_i\,,$$

$$I_{nml2}\Theta_{nml1,tt} + d_{nml2}\Theta_{nml1,t} + c_{nml1}l_{nml1}\Theta_{nml1,xt} +$$
$$+k_{nml1}l_{nml1}\Theta_{nml1,x} = M_{nml21}(t) \qquad \text{for } x = \sum_{j=1}^{nml1} l_j\,,$$

where:

$$L_i(\Theta_i(t)) = \frac{\mathrm{d}I_i(\Theta_i(t))}{\mathrm{d}(\Theta_i(t))}\,, \qquad i = 2,\,3,\ldots\,,n+1,$$

$$\Delta\Theta_k(t) = \alpha_k\Theta_k^{(1)}(t) - \beta_k\Theta_k^{(2)}(t)\,, \qquad k = n+2,\,n+3,\ldots\,,n+m+1,$$

and d_j, c_l are constant external and internal damping coefficients, respectively, i. e. $j = 1,\,2,\,\ldots,\,n+m+l+2$, $l = 1,\,2,\,\ldots,\,n+m+l+1$. However, functions $e_k(\Delta\Theta_k(t))$ and $h_k(\Delta\Theta_k(t))$ denote non-linear damping and stiffness coefficients, respectively, for the elastic coupling, gear stages and joints. Coefficients α_k and β_k are radii of the driving and driven

gear wheels, respectively, for the case of gear stages. However, for the elastic coupling, friction clutch and the Cardan universal joints α_k and β_k are equal to unity. Superscripts (1) and (2) are assigned to respective quantities corresponding to the driving and driven elements in the system, $nml2 = n + m + l + 2$, $nml1 = n + m + l + 1$, and the subscripts after commas denote partial differentiations.

Solutions of equations (2) are sought in the form of d'Alembert wave solutions

$$\begin{aligned}
&\Theta_1(x,t) = f_1(at - x + l_1) + g_1(at + x - l_1)\,,\\
&\Theta_i(x,t) = f_i\left(at - x + \sum_{j=1}^{i-1} l_j\right) + g_i\left(at + x - \sum_{j=1}^{i-1} l_j\right)\,,\\
&\qquad i = 2,\,3,\,\ldots\,,\,n+1\,,\\
&\Theta_k(x,t) = f_k\left(at - x + \sum_{j=1}^{n-1} l_j\right) + g_k\left(at + x - \sum_{j=1}^{n-1} l_j - 2\sum_{j=n}^{k-1} l_j\right)\,,\\
&\qquad k = n+2,\,\ldots\,,\,n+m+l+1\,.
\end{aligned} \tag{3}$$

Functions f_i and g_i in (3) represent torsional waves propagating in the elastic elements as a result of the external torque application. They are determined by the boundary and initial conditions [7, 8, 10, 11]. Thus, substituting (3) into the boundary conditions (2) leads to the following system of linear and non-linear ordinary differential equations with a 'shifted' argument z for functions f_i and g_i, $i = 1, 2, \ldots, n+m+l+1$,

$$r_{21}f_1''(z) + r_{11}f_1'(z) = M_1(z) + s_{21}g_1''(z - 2l_1) + s_{11}g_1'(z - 2l_1)\,,$$

$$r_{2,nml2}g''_{nml1}(z) + r_{1,nml2}g'_{nml1}(z) =$$

$$= M_{nml2}(z) + s_{2,nml2}f''_{nml1}(z - 2l_{nml1}) + s_{1,nml2}f'_{nml1}(z - 2l_{nml1})\,,$$

$$g_i'(z) = -f_i'(z - 2l_i) + f_{i+1}'(z - l_i) + g_{i+1}'(z - l_i)\,, \qquad i = 2,\,3,\,\ldots\,,\,n\,,$$

$$g_j'(z) = -f_j'(z - 2l_j) + f_{j+1}'(z - 2l_j) + g_{j+1}'(z - 2l_j)\,,$$

$$j = n+m+1,\,n+m+2,\ldots\,,\,n+m+l\,,$$

$$r_{22}(z)f_2''(z) + r_{12}(z)f_2'(z) = M_2(z) + s_{22}(z)g_2''(z) +$$

$$+ s_{12}(z)g_2'(z) + t_{22}f_1''(z) + t_{12}f_1'(z)\,,$$

$$r_{2i}(z)f_i''(z) + r_{1i}(z)f_i'(z) = M_i(z) + s_{2i}(z)g_i''(z) +$$

$$+ s_{1i}(z)g_i'(z) + t_{2i}f_{i-1}''(z - l_{i-1}) + t_{1i}f_{i-1}'(z - l_{i-1})\,, \qquad i = 3,\,4,\,\ldots\,,\,n+1\,,$$

$$\begin{bmatrix} p_{2,k-1} & 0 \\ 0 & r_{2,k} \end{bmatrix} \begin{bmatrix} g''_{k-1}(z+2l_{k-1}) \\ f''_k(z) \end{bmatrix} +$$

$$\begin{bmatrix} p_{1,k-1}(z) & -\alpha_k\beta_k e_k(\Delta_k(z)) \\ -\alpha_k\beta_k e_k(\Delta_k(z)) & r_{1,k}(z) \end{bmatrix} \begin{bmatrix} g'_{k-1}(z+2l_{k-1}) \\ f'_k(z) \end{bmatrix} +$$

$$+ \begin{bmatrix} \alpha_k^2 h_k(\Delta_k(z)) & -\alpha_k\beta_k h_k(\Delta_k(z)) \\ -\alpha_k\beta_k h_k(\Delta_k(z)) & \beta_k^2 h_k(\Delta_k(z)) \end{bmatrix} \begin{bmatrix} g_{k-1}(z+2l_{k-1}) \\ f_k(z) \end{bmatrix} =$$

$$= \begin{bmatrix} M_k^{(1)}(z) + u_{2,k-1} f''_{k-1}(z) + u_{1,k-1}(z) f'_{k-1}(z) + \\ M_k^{(2)}(z) + s_{2,k} g''_k(z) + s_{1,k}(z) g'_k(z) + \end{bmatrix}$$

$$\begin{bmatrix} +\alpha_k\beta_k e_k(\Delta_k(z))\, g'_k(z) + \alpha_k h_k(\Delta_k(z)) [\beta_k g_k(z) - \alpha_k f_{k-1}(z)] \\ +\alpha_k\beta_k e_k(\Delta_k(z))\, f'_{k-1}(z) - \beta_k h_k(\Delta_k(z)) [\beta_k g_k(z) - \alpha_k f_{k-1}(z)] \end{bmatrix},$$

$$\Delta_k(z) = \alpha_k [f_{k-1}(z) + g_{k-1}(z+2l_{k-1})] - \beta_k [f_k(z) - g_k(z)],$$

$$k = n+2,\ n+3,\ \ldots,\ n+m+1,$$

$$r_{2j} f''_j(z) + r_{1j} f'_j(z) = M_j(z) + s_{2j} g''_j(z) + s_{1j} g'_j(z) + t_{2j} f''_{j-1}(z) + t_{1j} f'_{j-1}(z),$$

$$j = n+m+2,\ n+m+3,\ \ldots,\ n+m+l+1,$$

$$g'_1(z) = -f'_1(z) + f'_2(z) + f'_2(z), \tag{4}$$

where:

$$r_{21} = c_1 l_1 + a I_1, \qquad r_{11} = \frac{l_s (k_1 l_1 + a d_1)}{a},$$

$$s_{21} = c_1 l_1 - a I_1, \qquad s_{11} = \frac{l_s (k_1 l_1 - a d_1)}{a},$$

$$r_{2,nml2} = c_{nml1} l_{nml1} + a I_{nml2}, \qquad r_{1,nml2} = \frac{l_s (k_{nml1} l_{nml1} + a d_{nml2})}{a},$$

$$s_{2,nml2} = c_{nml1} l_{nml1} - a I_{nml2}, \qquad s_{1,nml2} = \frac{l_s (k_{nml1} l_{nml1} - a d_{nml2})}{a},$$

$$r_{2i}(z) = c_i l_i + c_{i-1} l_{i-1} + a I_i(z),$$

$$r_{1i}(z) = \frac{l_s [k_i l_i + k_{i-1} l_{i-1} + a (d_i + \Omega_i(z) L_i(z))]}{a},$$

$$s_{2i}(z) = c_i l_i - c_{i-1} l_{i-1} - a I_i(z),$$

$$s_{1i}(z) = \frac{l_s [k_i l_i - k_{i-1} l_{i-1} - a (d_i + \Omega_i(z) L_i(z))]}{a},$$

$$t_{2i} = 2 c_{i-1} l_{i-1}, \qquad t_{1i} = \frac{2 k_{i-1} l_{i-1} l_s}{a}, \qquad \Omega_i(z) = 0.5 \left[f'_i(z) + g'_i(z) \right],$$

$$i = 2,\ 3,\ \ldots,\ n+1,\ n+m+2,\ n+m+3,\ \ldots,\ n+m+l+1,$$

$$p_{2,k-1} = c_{k-1} l_{k-1} + a I_k^{(1)},$$

$$p_{1,k-1}(z) = \frac{l_s \left[k_{k-1} l_{k-1} + a \left(d_k^{(1)} + \alpha_k^2 e_k \left(\Delta_k(z) \right) \right) \right]}{a},$$

$$u_{2,k-1} = c_{k-1} l_{k-1} - a I_k^{(1)},$$

$$u_{1,k-1}(z) = \frac{l_s \left[k_{k-1} l_{k-1} - a \left(d_k^{(1)} - \alpha_k^2 e_k \left(\Delta_k(z) \right) \right) \right]}{a},$$

$$r_{2,k} = c_k l_k + a I_k^{(2)}, \qquad r_{1,k}(z) = \frac{l_s \left[k_k l_k + a \left(d_k^{(2)} + \beta_k^2 e_k \left(\Delta_k(z) \right) \right) \right]}{a},$$

$$s_{2,k} = c_k l_k - a I_k^{(2)}, \qquad s_{1,k}(z) = \frac{l_s \left[k_k l_k - a \left(d_k^{(2)} - \beta_k^2 e_k \left(\Delta_k(z) \right) \right) \right]}{a},$$

$$k = n+2, n+3, \ldots, n+m+1$$

and l_s is an arbitrary value. Using the Newmark method to solve (4) together with (3), one obtains system transient or steady-state dynamic response in the form of tangential stresses, torques, angular velocities, accelerations and displacements of arbitrary cross-sections of the hybrid model elastic elements. The 'shifted' argument in *Eqs.* (4), which is a consequence of the wave interpretation of torsional vibrations, makes their right hand sides always known in each step of computation. Thus, in contrary to the coupled ordinary differential equations for the discrete model, it is possible to solve *Eqs.* (4) sequentially, one after another, in presented order. This feature very essentially simplifies the numerical procedure. Results obtained by using the proposed wave approach for the crank mechanisms of the internal combustion reciprocating engines were compared in [7, 8, 10] with the analogous results yielded by the so far applied methods based on the discrete model. From these comparisons, it follows that using the wave method one obtains better numerical stability and accuracy of results, but first of all — much higher numerical efficiency, where the computation time was reduced from 2.5 to 10 times down and more.

3. Numerical Results

In the presented paper, numerical calculations were performed for two exemplary geared drive systems of the rail and motor vehicles.

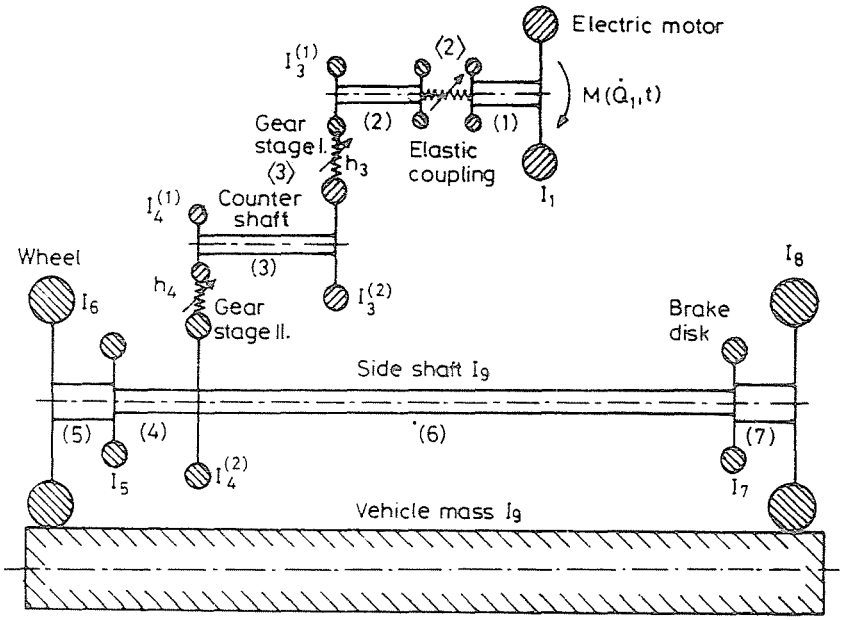

Fig. 3. Discrete-continuous model of the electric locomotive bogie drive system

a) Run-Up Simulation of the Rail Vehicle Drive System

In this example, there was performed a run-up of the electric locomotive. The drive system of it consists of the electric motor, elastic coupling with progressive characteristic, two gear stages, bogie wheelset with two brake disks and the locomotive mass. The discrete-continuous model of this system is shown in *Fig. 3.* In this model, a numerical value of the 'vehicle mass' is a fraction of the total locomotive mass divided by the number of wheelsets, because identical reaction forces between the locomotive wheels and rails are assumed. Moreover, a rolling contact between the driven wheels and rails is assumed. Thus, the rigid bodies of mass moments of inertia I_6 and I_8 representing wheels as well as the rigid body of mass moment of inertia I_9 representing the 'vehicle mass' are regarded as one rigid body of the total mass moment of inertia $I_6 + I_8 + I_9$. According to *Eqs.* (2), this drive system model is characterized by the following parameters: $n = 0$, $m = 3$ and $l = 2$. There are assumed backlashes in the gear stages and a harmonic variation of the mesh stiffnesses due to a variable number of teeth in contact [1].

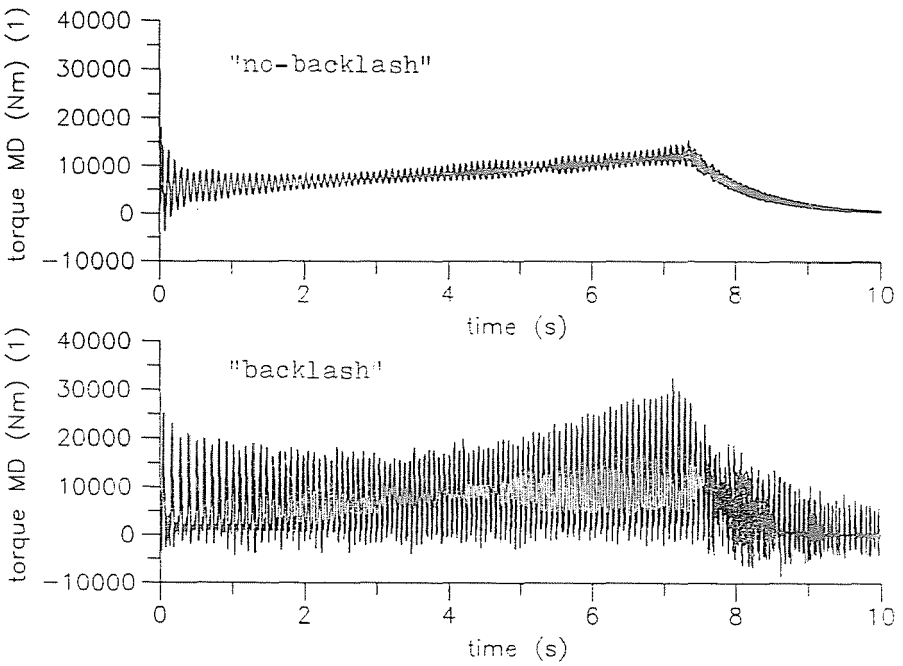

Fig. 4. Dynamic torque in the motor output shaft (1)

There is performed a simulation of a locomotive acceleration from its standstill lasting for 10 seconds. *Fig. 4* shows plots of the dynamic torque transmitted by the elastic element (1) corresponding to the motor output shaft for two cases: with 'no backlash' assumed and with 'backlash' in both gear stages, respectively. As one can notice, backlashes in the gear stages cause a very essential increase in dynamic torque pulsating component. However, *Fig. 5* shows plots of the dynamic torque transmitted by the second gear stage (4). The response obtained for 'no backlash' in the gear stage is a superposition of the 'quasi-harmonic' pulsating component and the quasi-static component generated by the electric motor. But the torque history for the 'backlash' case is a series of successive peaks due to impacts of teeth according to the assumed gear mesh characteristics. It should be noted that the maximum peak values are always positive ones, and they are much smaller in a comparison with the extreme values of the torque history for the 'no backlash' case (*Fig. 5.*) However, for a change, the successive impacts of teeth mentioned above induce incomparably greater instantaneous angular accelerations of the driven gear wheel in comparison with the 'no backlash' case (*Fig. 6.*) Thus, due to a superposition of the elastic and inertia forces in the gear stage, the resultant dynamic torque

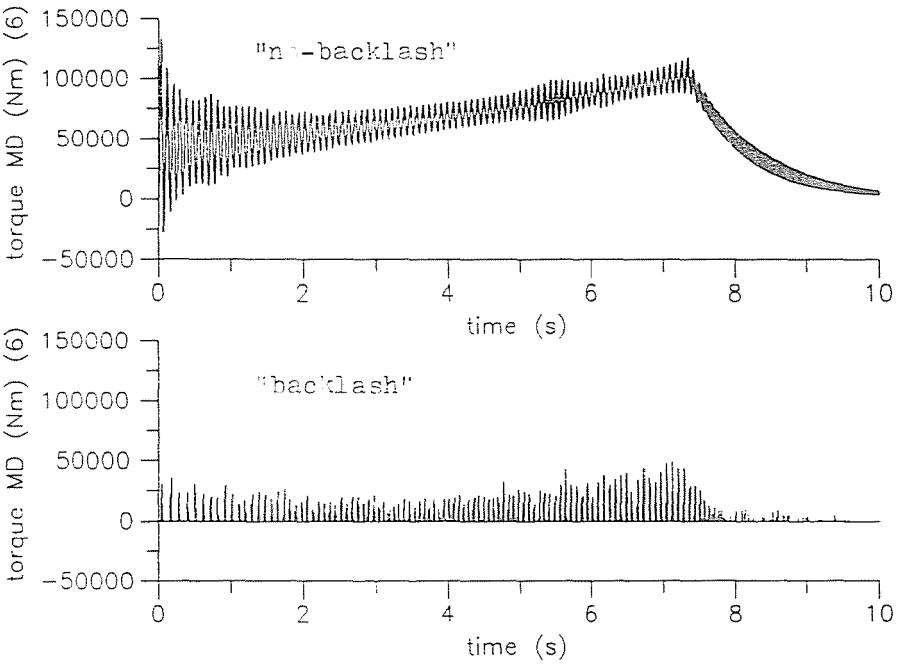

Fig. 5. Dynamic torque in the second gear stage (4)

transmitted by the output side shaft (6) for the 'backlash' case is characterized by greater extreme values than the dynamic torque for the 'no backlash' case (*Fig. 7.*) Analogous results were obtained for the first gear stage (3).

From the above example it follows that a consideration of backlashes in the gear stages very essentially influences the results of the vibration process in the drive system both quantitatively and qualitatively. But for the parameters assumed in calculations, an influence of the gear mesh stiffness variation due to variable number of teeth in contact is of a secondary importance.

b) Run-Up Simulation of the Motor Vehicle Drive System

The considered drive system of the motor vehicle consists of the crank mechanism of the 6 cylinder in-line carburettor engine, flywheel, elastic coupling, three gear stages, rear driven wheels and the vehicle mass which are mutually connected by means of shaft segments and flexible elements. In comparison with the previous example, the discrete-continuous model of this system presented in *Fig. 8* is characterized by $n = 6$, $m = 4$ and

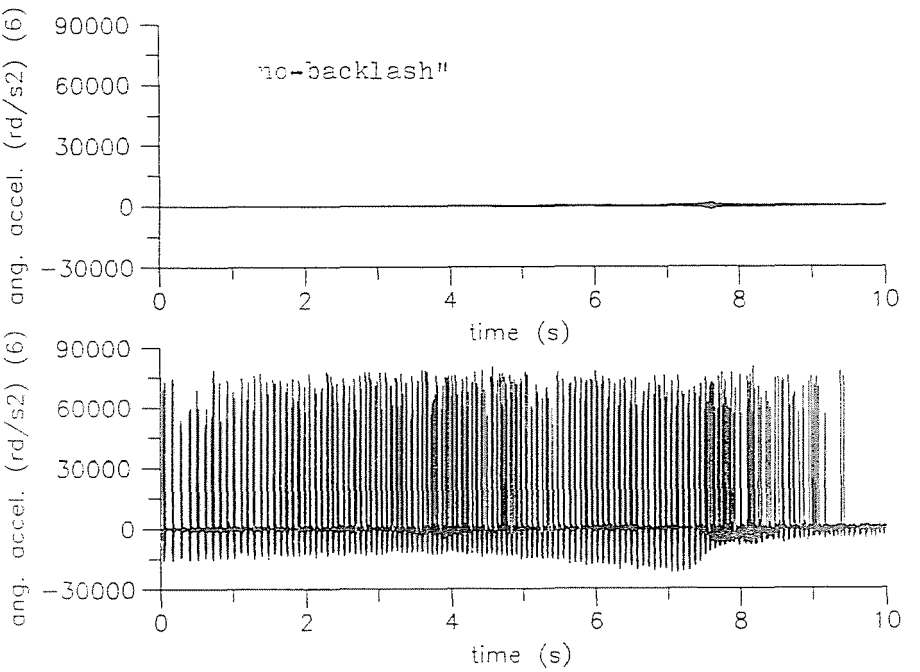

Fig. 6. Angular acceleration of the second gear stage driven gear wheel

$l = 3$. In this figure, the elastic elements (13) and (15) represent equivalent torsional flexibilities of tyres. The system is excited to vibrations by the active torques due to engine gas and inertia forces as well as by the passive torque due to drag force. The characteristic of the elastic coupling is assumed linear with dry friction [1]. However, for gear stage meshings, classical linear elastic characteristics with backlashes are assumed [1, 2].

The system was accelerated from the crankshaft average rotation speed 1000 [rpm] to 6000 [rpm] due to the constant mean gas torque value equal to 120 [Nm]. *Fig. 9* shows the history of the dynamic torque transmitted by the final 7th crankshaft journal within the time and frequency domains. From the presented plot it follows, that the system passes through a severe resonance corresponding to the 'first crankshaft' natural frequency 386.2 [Hz] with a node near the flywheel. However, *Fig. 10* presents plots of the dynamic torque transmitted by the elastic coupling, i. e. at the engine output. The obtained time domain plot of the attenuated sinusoidal shape is characterized by relatively small extreme values in comparison with those in *Fig. 9* and by the small 'fundamental' frequency corresponding to the first system natural frequency 2.1 [Hz]. *Fig. 11* shows a plot of the dynamic torque transmitted by the first gear stage (9) for the assumed

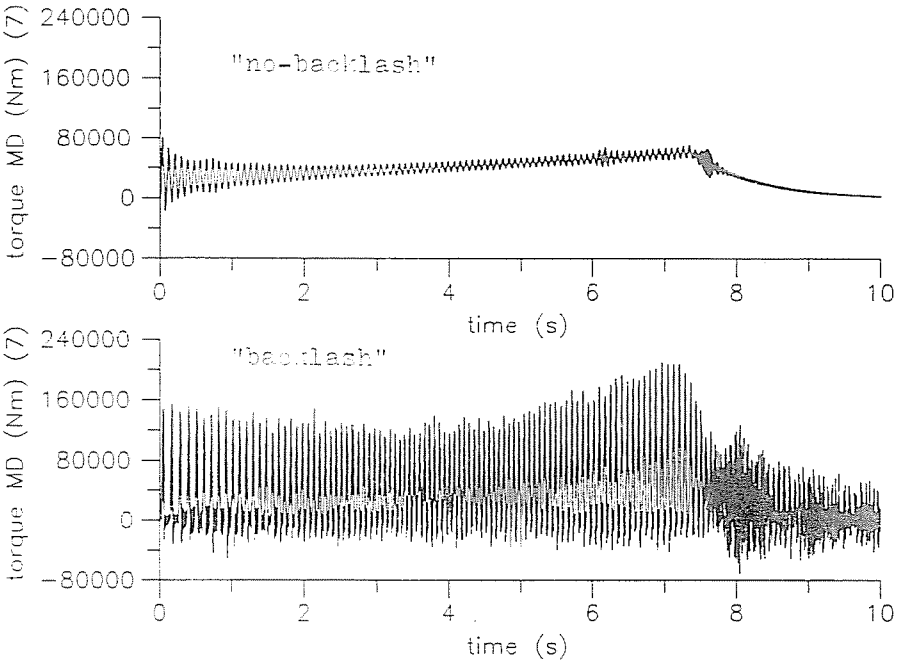

Fig. 7. Dynamic torque in the side shaft (6)

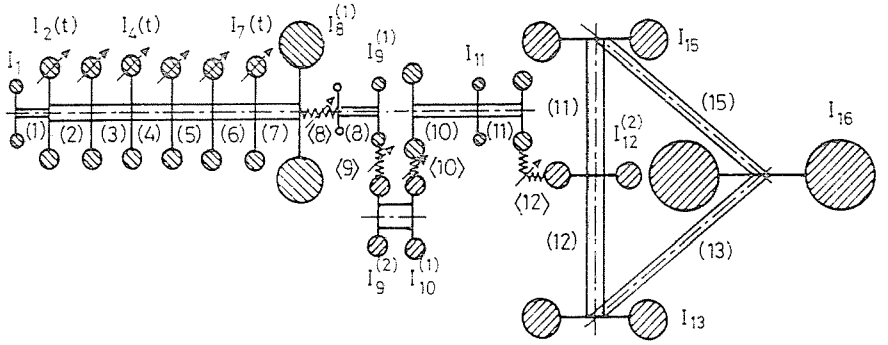

Fig. 8. Discrete-continuous model of the motor vehicle drive system

relatively small meshing stiffness value in contact, i. e. comparable with the torsional stiffness of the gearbox input shaft (8). A shape of the curve in *Fig. 11* is similar to that in *Fig. 10,* which indicates that the influence of backlash in this gear stage is very weak. But *Fig. 12* presents a history of the dynamic torque in the time and frequency domains transmitted by

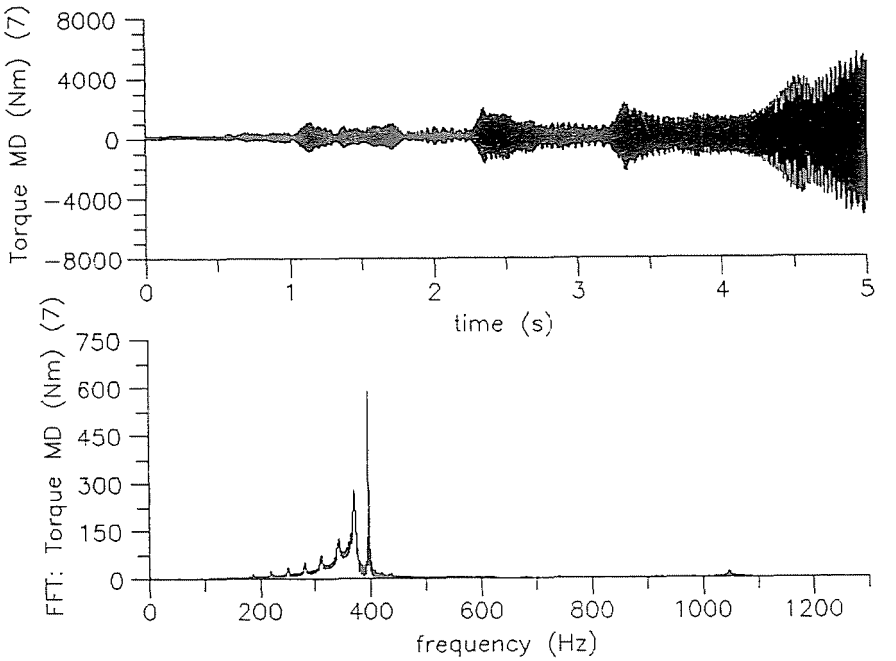

Fig. 9. Dynamic torque in the 7th crankshaft-journal (7)

the second gear stage (10). The meshing stiffness in contact for this stage is assumed ten times greater than that for the first gear stage (9). In this case, the system response is of a completely different character, where the obtained plot in the time domain is a series of sharp peaks corresponding to successive gear tooth impacts according to the gear mesh characteristic with backlash. This response in the frequency domain is characterized by high frequency components. Due to the superposition of dynamic torques of the elastic and inertia forces mentioned in the previous example, a curve of the dynamic torque transmitted in the side shafts (12) and (14) has a smooth attenuated sinusoidal form oscillating around the static drive torque value (*Fig. 13.*)

4. Final Remarks

In the paper, there is presented an alternative technique for the numerical simulation of non-linear torsional vibrations in the motor and rail vehicle drive systems. This technique is on a discrete-continuous (hybrid) mechanical model and on the one-dimensional wave description of vibration process. In the mathematical model, all non-linear effects are contained in

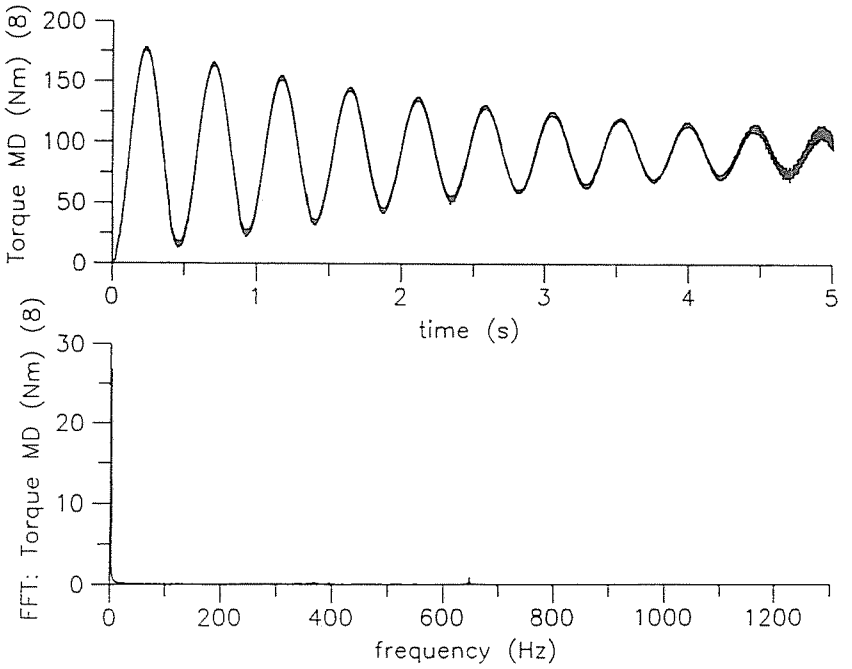

Fig. 10. Dynamic torque in the elastic coupling (8)

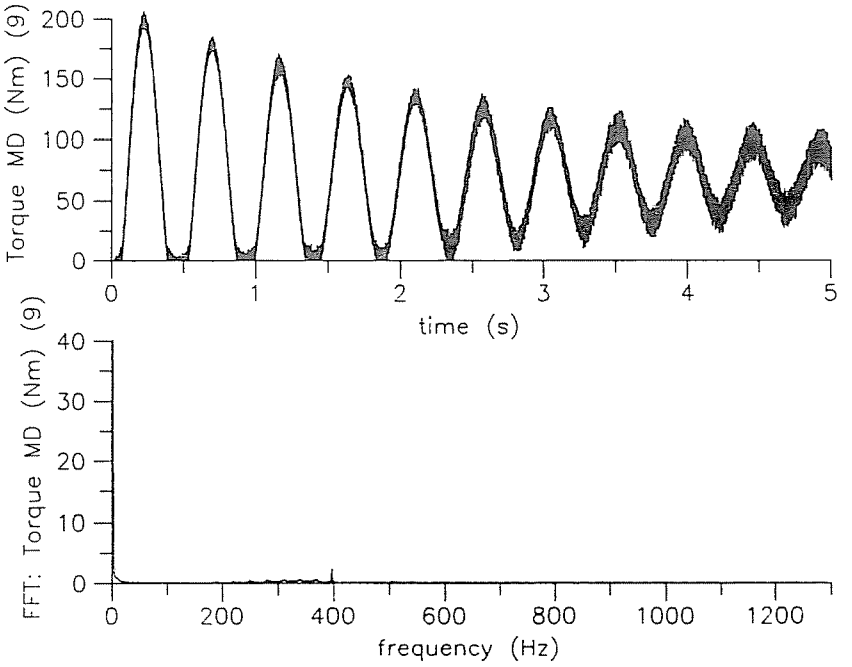

Fig. 11. Dynamic torque in the first gear stage (9)

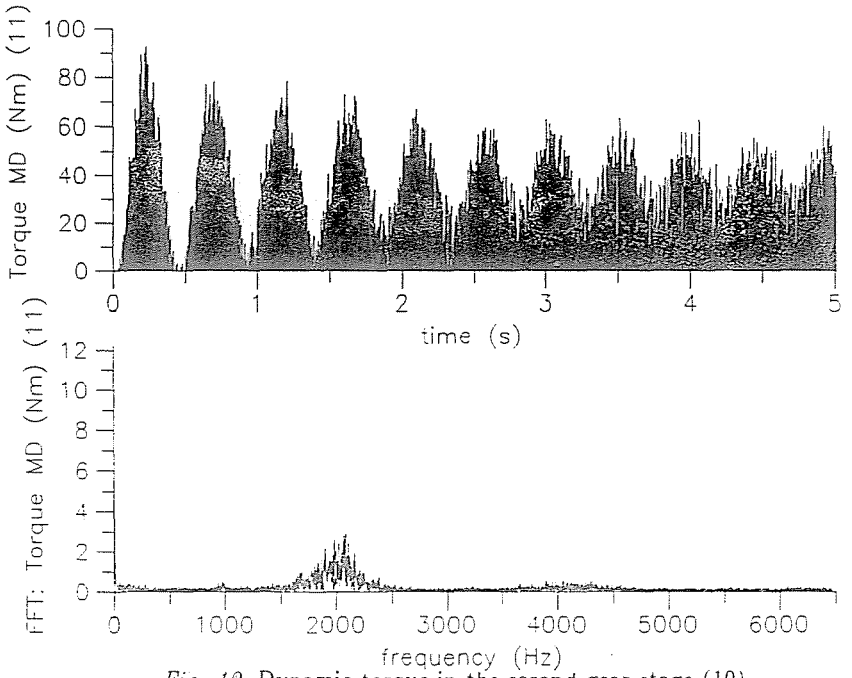

Fig. 12. Dynamic torque in the second gear stage (10)

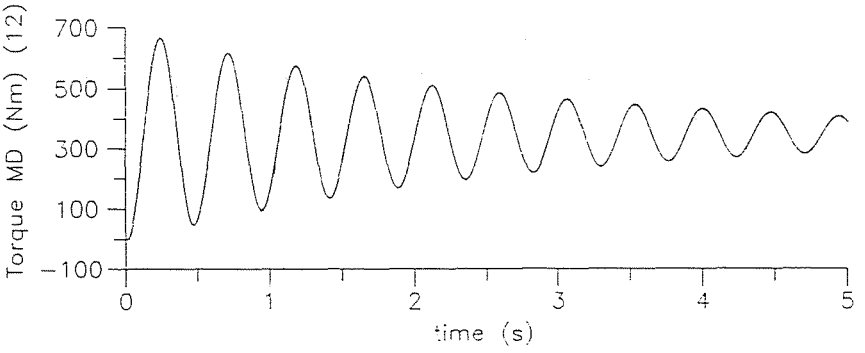

Fig. 13. Dynamic torque in the side shafts (12) and (14)

the equations of boundary conditions. The proposed numerical procedure is much more efficient and accurate in comparison with the so far existing procedures based on analogous discrete mechanical models.

In the numerical examples, there were performed run-up simulations of the electric locomotive and motor vehicle drive systems. Attention was paid to the influence of the gear mesh parameters on the system dynamic

response, in particular, how sensitive the responses were to these parameters. The importance of the appropriately assumed gear mesh characteristics was proved for histories of dynamic torques transmitted by such drive system elements like the gear stages and shaft segments.

References

1. LASCHET, A.: Simulation von Antriebssystemen, Springer-Verlag, 1988.
2. NERIYA, S. V. – BHAT, R. B. – SANKAR, T. S.: On the Dynamic Response of a Helical Geared System Subjected to a Static Transmission Error in the Form of Deterministic and Filtered White Noise Inputs, *Proc. of the 11th Biennial ASME Conf. on Mechanical Vibration and Noise, ASME Rotating Machinery Dynamics*, DE-Vol. 2. pp. 287–296. Boston, USA, 1987.
3. KUBO, A.: On Analysis and Prediction of Machine Vibration Caused by Gear Meshing, *Proc. of the 4th World Congress on the Theory of Machines and Mechanisms*, Sevilla, Spain, 1987, Pergamon Press, Vol. 3. pp. 1355–1358.
4. CHOU, J. J. – YANG, D. C. H.: Free Impact Frequency Estimation for Meshing Gears, *Proc. of the 7th World Congress on the Theory of Machines and Mechanisms*, Sevilla, Spain, 1987, Pergamon Press, Vol. 2. pp. 815–819.
5. PFEIFFER, F. – KUNERT, A.: Rattling Models from Deterministic to Stochastic Processes, *Nonlinear Dynamics*, Kluwer Academic Publishers, Vol. 1. No. 1. pp. 63–74, 1990.
6. EVANS, B. F. – SMALLEY, A. J. – SIMONS, H. R.: Startup of Synchronous Motor Drive Trains: the Application of Transient Torsional Analysis to Cumulative Fatigue Assessment, *Trans. of the ASME*, Paper No. 85-DET-122.
7. BOGACZ, R. – IRRETIER, H. – SZOLC, T.: On Discrete-continuous Modelling of the Rotating Systems for a Non-linear Torsional Vibration Analysis, *Proc. of the International Conference on Rotating Machine Dynamics, 'Rotordynamics '92'*, Venice, April 1992, Springer-Verlag, Michael J. Goodwin (Ed.), pp. 240–247.
8. BOGACZ, R. – SZOLC, T.: Non-linear Torsional Vibration Analysis of the Drive Systems Using the One-dimensional Elastic Waves, *Archives of Mechanics*, 1993, (in print).
9. SZOLC, T. – BOGACZ, R. – IRRETIER, H.: Parameter Identification of a Hybrid Model for Vibration Analysis Using the Finite Element Method, *Z. angew. Math. Mech.*, Vol. 71, 1991, 4, T 207–T 209.
10. SZOLC, T.: Modelling of the Crank Mechanisms of Internal Combustion Engines Using the Torsional Elastic Waves, *Doctoral Dissertation*, Inst. of Fundamental Technological Research, Warsaw 1985, (in Polish).
11. BOGACZ, R. – SZOLC, T. – IRRETIER, H.: An Application of Torsional Wave Analysis to Turbogenerator Rotor Shaft Response, *Trans. of the ASME, Journal of Vibration and Acoustics*, April 1992, Vol. 114, pp. 149–153.